Earth Surf. Dynam. Discuss., 3, 1289–1316, 2015
www.earth-surf-dynam-discuss.net/3/1289/2015/
doi:10.5194/esurfd-3-1289-2015

Earth Surface Dynamics
Discussions
Open Access

Morphology of meandering and braided gravel-bed streams from the Bayanbulak Grassland, Tianshan, China

F. Métivier[1], O. Devauchelle[1], H. Chauvet[1], E. Lajeunesse[1], P. Meunier[2], K. Blanckaert[3], Z. Zhang[4], Y. Fan[5], Y. Liu[6], Z. Dong[4], and B. Ye[4]

[1]Institut de physique du globe de Paris – Sorbonne Paris Cité, Université Paris Diderot, CNRS, UMR7154, 1 Rue Jussieu, 75238 Paris CEDEX 05, France
[2]Département de Géologie, UMR8538, CNRS, Ecole Normale Supérieure, 24 Rue Lhomond, 75005 Paris, France
[3]Research Center for Eco-Environmental Sciences, Chinese Academy of Sciences, Beijing, China
[4]The States Key laboratory of Cryospheric Science, Cold and Arid Region Environmental and Engineering and Research Institute, Chinese Academy of Sciences, 260 Donggang West Road, Lanzhou, China
[5]Xinjiang Institute of Ecology and Geography, Chinese Academy of Sciences, Urumqi, China
[6]Key Laboratory of Water Environment and Resource, Tianjin Normal University, 393 Binshui West Road, Tianjin 300387, China

Received: 12 October 2015 – Accepted: 16 October 2015 – Published: 13 November 2015

Correspondence to: F. Métivier (metivier@ipgp.fr)

Published by Copernicus Publications on behalf of the European Geosciences Union.

Abstract

The Bayanbulak Grassland, Tianshan, China is located in an intramountane sedimentary basin where meandering and braided gravel-bed streams coexist under the same climatic and geological settings. We report on measurements of their discharge, width, depth, slope and grain size. Based on this data set, we compare the morphology of individual threads from braided and meandering streams. Both types of threads share statistically indistinguishable regime relations. Their depths and slopes compare well with the threshold theory, but they are wider than predicted by this theory. These findings are reminiscent of previous observations from similar gravel-bed streams. Using the scaling laws of the threshold theory, we detrend our data with respect to discharge to produce a homogeneous statistical ensemble of width, depth and slope measurements. The statistical distributions of these dimensionless quantities are similar for braided and meandering streams. This suggests that a braided river is a collection of intertwined channels, which individually resemble isolated streams. Given the environmental conditions in Bayanbulak, we furthermore hypothesize that bedload transport causes the channels to be wider than predicted by the threshold theory.

1 Introduction

The morphology of alluvial rivers extends between two end members: in meandering rivers, the flow of water and sediments is confined in a single channel, whereas in braided rivers the flow is distributed into intertwined threads separated by bars (Schumm, 2005). Linear stability analyses, supported by laboratory experiments, explain how bedload transport generates bars, which in turn can grow into a fully developped braided parttern (Parker, 1976; Fredsøe, 1978; Zolezzi et al., 2012). This mechanism proves more efficient in wide and shallow channels. Field measurements indicate that the bankfull aspect ratio of braided rivers is usually much larger that that of meandering ones, thus suggesting that the bar instability is indeed responsible for braiding (Parker, 1976; Fredsøe, 1978; Zolezzi et al., 2012). What exactly controls the aspect ratio of an alluvial river remains an open question, although sediment discharge and riparian vegetation are significant in this respect: high sediment load and weak vegetation favour wider and shallower channels, and often induce braiding (Smith and Smith, 1984; Gran and Paola, 2001; Tal and Paola, 2007, 2010; Metivier and Barrier, 2012).

In a fully developed braided river, emerged bars separate the threads from each other, and the very definition of bankfull conditions becomes ambiguous. Most authors treat the river as a whole by defining lumped quantities, such as the total river width or the average water depth (Metivier and Barrier, 2012). Conversely, a few studies consider the morphology of individual threads, and compare it to isolated channels (Church and Gilbert, 1975; Mosley, 1983; Gaurav et al., 2015). In sandy braided rivers, the morphology of individual threads appears to be indistinguishable from that of isolated streams from the same environment. This observation accords with recent laboratory experiments (Seizilles et al., 2013; Reitz et al., 2014). To our knowledge, this similarity has not been investigated in gravel-bed braided rivers.

Here, we report on measurements in the Bayanbulak Grassland, Tianshan Mountains, China, where tens of meandering and braided gravel-bed rivers develop in the same environment. After comparison with other datasets from the literature, we compare the morphology of braided and meandering threads in our dataset. Finally, we rescale our measurements based on the threshold theory to generate a single statistical ensemble from streams highly dispersed in size (Glover and Florey, 1951; Henderson, 1963; Seizilles et al., 2013; Gaurav et al., 2015).

2 Field site

The Bayanbulak grassland is an intramontane sedimentary basin standing at an elevation of about 2500 m in the Tianshan Mountains (Fig. 1). Two main wetlands, the Qong Yulduz basin (known as the Swan Lake in Chinese) and the Kizik Yulduz basin, are distributed around the main Kaidu River. They are immediately surrounded by gently sloping meadows (slope $S \sim 0.01$), themselves enclosed with the Tianshan Mountains which provide water to the Kaidu River (Zhang et al., 2002). The hydrology of the basins is controlled by snowmelt and summer orographic precipitations (Zhang et al., 2002; Yang and Cui, 2005). Snow accumulates from November to March, and starts melting in April, inducing the water discharge to rise in all streams (Zhang et al., 2007). Orographic precipitation takes over in summer (between 260 and 290 mm), and the discharge continues to rise until August (Fig. 5).

The morphology of the Bayanbulak streams varies between highly meandering and braided, and the same river often switches from one to the other (Figs. 2 and 3). The streams span about four orders of magnitude in discharge, and about two in width (Fig. 4). Various species of grass dominate the vegetation over the entire basins, and their influence on the morphology of the streams is certainly only mild (Zhang et al., 2002; Hey and Thorne, 1986). Finally, most streams flow over gravel, which size distribution does not vary significantly over the basins (Fig. 4). All these features combine to make the Bayanbulak grassland an ideal field site to investigate the morphology of gravel-bed rivers.

3 Method

To compare the morphology of braided and meandering threads, we carried out two field campaigns in July 2012 and July 2013, during the high-flow season (Fig. 5). We treated the threads of braided rivers as individual channels, based on the wetted area at the time of measurement. We measured the cross-section geometry, the discharge, the grain-size distribution and the slope of as many streams, spanning as broad a range in discharge, as possible.

To measure the cross section and the water discharge of large streams, we used a 2Mhz acoustic Doppler current profiler (ADCP, Teledyne-RDI StreamPro). In shallower streams, we used wading rods, rulers and floats to measure the surface velocity, and estimated the vertically-averaged velocity from it (Sanders, 1998; Gaurav et al., 2015). Repeated ADCP profiles across the same section show that discharge, width and depth measurements are all reproducible within less than 15 %. Manual measurements yields an uncertainty of about 2 % for width, 12 % for depth and 25 % for velocity. The resulting uncertainty on discharge is less than 40 % for both methods.

We used a Topcon theodolite with a laser rangefinder to measure the long profile of the streams, and estimate their slope. Uncertainties on the location of the total station and atmospheric inhomogeneities curtail the precision of long-distance profiles. For our measurements, we expect the uncertainty on angle to reach 90″. The corresponding absolute uncertainty on the slope of a river is about 5×10^{-4}.

Finally, we measured the grain-size distribution from surface counts (Bunte and Abt, 2001), and extracted the median grain size d_{50} and the size of the 90th percentile d_{90} from these distribution.

Overall, our dataset is composed of 92 measurements of width, depth, average velocity, discharge, slope and grain size, among which 53 correspond to braided-river threads (Table 3), and 39 to meandering threads (Table 4).

4 Regime equations

Figure 4 compares our measurements to three sources: the compendiums of Parker et al. (2007); Church and Rood (1983) and King et al. (2004), hereafter referred to as GBR. All streams from the GBR dataset are isolated (non braided) threads.

The Bayanbulak streams are widely dispersed in size ($0.6 \leq W \leq 77$ m), and discharge ($0.002 \leq Q \leq 100\,\mathrm{m^3\,s^{-1}}$). On average, they are smaller than the GBR streams. Similarly, their average grain-size $d_{50} \simeq 0.013$ m is finer (the standard deviation of the d_{50} is $\sigma_{d_{50}} \sim 0.008$ m). Our dataset therefore extend the GBR one towards smaller channels.

We now consider the empirical regime equations of individual threads (Fig. 6). To facilitate the comparison between the GBR streams and our own, we use dimensionless quantities, namely W/d_{50}, H/d_{50}, S and $Q_* = Q/\sqrt{gd_{50}^5}$, where g is the acceleration of gravity. Not surprisingly, the morphology of a thread is strongly correlated with its water discharge: its width and depth increase with discharge, while its slope decreases. At first sight, these trends are similar for isolated and braided threads. They also compare well to the GBR data set, although the Bayanbulak streams are slightly wider than the GBR ones on average. The measurement uncertainty, although significant, is less than the variability of our data, except for slopes smaller than about 5×10^{-3} (Sect. 4).

Despite considerable scatter, our measurements gather around straight lines in the log-log plots of Fig. 6, suggesting power-law regime equations:

$$\frac{W}{d_{50}} = \alpha_\mathrm{w} Q_*^{\beta_\mathrm{w}} \ ; \quad \frac{H}{d_{50}} = \alpha_\mathrm{h} Q_*^{\beta_\mathrm{h}} \ ; \quad S = \alpha_\mathrm{s} Q_*^{\beta_\mathrm{s}} \tag{1}$$

where α_w, α_h, α_s, β_w, β_h and β_s are dimensionless parameters. To evaluate them, we use reduced major axis regression (RMA) instead of least square regression because the variability of our data is comparable along both axis (Sokal and Rohlf, 1995; Scherrer, 1984). The resulting fitted coefficients are reported in Table 1. The scatter in the slope measurement is too large to provide significant estimates of the slope coefficients α_s and β_s. At the 95 % confidence level, the regime relationships of meandering and braided threads cannot be distinguished. Similarly, the depth of the Bayanbulak streams cannot be distinguished from those of the GBR ones. Conversely, the Bayanbulak streams are significantly wider than the GBR ones.

So far we have made the width, depth and discharge dimensionless using d_{50} as the characteristic grain size of the sediment. This choice, however, is arbitrary (Parker et al., 2007; Parker, 2008). Large grains are arguably more likely to control the morphology of the river than smaller ones, and a larger quantile might be a better approximation of the characteristic grain size. For comparison, we rescaled our measurements using d_{90} instead of d_{50}, and repeated the above analysis. Our conclusions are not altered significantly by this choice of a characteristic grain size (Table 1).

5 Detrending

So far, we have found that the empirical regime equations of isolated and braided threads are statistically similar. To proceed further with this comparison, we would like to convert our measurements into a single statistical ensemble. We thus need to detrend our dataset with respect to water discharge, based on analytical regime equations. Following Gaurav et al. (2015), we propose to use the threshold theory to do so.

The threshold theory assumes that a river transports its sediment load slowly enough for is bed to be near the threshold of motion (Glover and Florey, 1951; Henderson, 1963; Yalin and Ferreira da Silva, 2001; Seizilles, 2013). Momentum and mass balances then yields power-law regime equations, the original formulation of which reads (Glover and Florey, 1951)

$$\frac{W}{d_s} = \left[\frac{\pi}{\sqrt{\mu}} \left(\frac{\theta_\mathrm{t}(\rho_\mathrm{s} - \rho)}{\rho} \right)^{-1/4} \sqrt{\frac{3C_\mathrm{f}}{2^{3/2}\mathcal{K}\left[1/2\right]}} \right] Q_*^{1/2}, \tag{2}$$

$$\frac{H}{d_s} = \left[\frac{\sqrt{\mu}}{\pi} \left(\frac{\theta_\mathrm{t}(\rho_\mathrm{s} - \rho)}{\rho} \right)^{-1/4} \sqrt{\frac{3\sqrt{2}C_\mathrm{f}}{\mathcal{K}\left[1/2\right]}} \right] Q_*^{1/2}, \tag{3}$$

$$S = \left[\left(\mu^{1/2} \frac{\theta_\mathrm{t}(\rho_\mathrm{s} - \rho)}{\rho} \right)^{5/4} \sqrt{\frac{\mathcal{K}\left[1/2\right] 2^{3/2}}{3C_\mathrm{f}}} \right] Q_*^{-1/2} \tag{4}$$

where

$$Q_* = \frac{Q}{\sqrt{g d_s^5}}, \tag{5}$$

is the dimensionless discharge. $\rho = 1000\,\mathrm{kg\,m^{-3}}$ and $\rho_\mathrm{s} = 2650\,\mathrm{kg\,m^{-3}}$ are the densities of water and sediment, $C_\mathrm{f} \approx 0.1$ is the turbulent friction coefficient, Q the water discharge, $\theta_\mathrm{t} \sim 0.04$ the threshold Shields parameter, $\mu \sim 0.7$ the friction angle for gravel, and $\mathcal{K}[1/2] \approx 1.85$ a transcendental integral (Glover and Florey, 1951; Henderson, 1963; Seizilles et al., 2013).

This formulation is similar to the one proposed by Parker et al. (2007), but for two points. First, Eqs. (2)–(4) represent a threshold channel, whereas Parker et al. (2007) extend the theory to active channels. Second, the formulation of Glover and Florey (1951) uses a constant friction coefficient in the momentum balance, whereas Parker et al. (2007) use a more elaborate friction law. Here we use the simplest formulation, as the variability of our data overshadows these differences (Metivier and Barrier, 2012).

The dashed line on Fig. 6 represents Eqs. (2)–(4). On average, the Bayanbulak streams are wider, shallower and steeper than the corresponding threshold channel. However, the theory predicts reasonably their dependence with respect to discharge, thus supporting its use to detrend our data. Accordingly, we define a set of rescaled quantities as follows:

$$W_* = \frac{W}{d_s C_\mathrm{W} \sqrt{Q_*}} = \frac{W (g d_s)^{1/4}}{C_\mathrm{W} \sqrt{Q}}, \tag{6}$$

$$H_* = \frac{H}{d_s C_\mathrm{H} \sqrt{Q_*}} = \frac{H (g d_s)^{1/4}}{C_\mathrm{H} \sqrt{Q}}, \tag{7}$$

$$S_* = S \frac{\sqrt{Q_*}}{C_\mathrm{S}} = \frac{S \sqrt{Q}}{g^{1/4} d_s^{5/4} C_\mathrm{S}}. \tag{8}$$

Here the coefficients C_W, C_H, C_S correspond to the prefactors in square brackets of Eqs. (2)–(4). We used the typical values reported above for the coefficients that do not vary in our dataset.

Figure 7 shows the relationship between the rescaled stream morphology and its dimensionless discharge, using d_{50} to approximate the characteristic grain size d_s. The new quantities W_*, H_* and S_* appear far less dependent on the water discharge than their original counterpart, although a residual trend remains for all of them. Using ordinary least squares, we fit power laws to our rescaled data to evaluate this residual trend. We find $W_* \propto Q_*^{-0.19\pm0.03}$ and $H_* \propto Q_*^{-0.10\pm0.05}$ for the Bayanbulak streams, and $W_* \propto Q_*^{-0.01\pm0.04}$ and $H_* \propto Q_*^{-0.16\pm0.04}$ for the GBR streams. The width of the Bayanbulak streams shows the strongest correlation, yet even this correlation is mild. Finally, slopes are more strongly correlated with discharge than width and depth both for the GBR streams ($S_* \propto Q_*^{0.21\pm0.05}$), and the Bayanbulak streams ($S_* \propto Q_*^{0.39\pm0.11}$). However, most of the difference between Bayanbulak and GBR streams is due to slopes well below the measurement precision. In all cases, the scatter is large, and all correlations fall within the standard deviation of the dataset.

6 Thread morphology

We now analyze our rescaled measurements as a homogeneous statistical ensemble (Fig. 7). The means of the rescaled width, depth and slope all fall about one order of magnitude away from one, and their dispersion around this mean is also about one order of magnitude (Table 2). This observation support the use of the threshold theory to scale the morphology of the Bayanbulak streams.

The dispersion of the rescaled slope is more significant than that of width and depth. We believe that, in addition to the technical difficulties associated to the measurement of slope in the field (Sect. 3), the dispersion of the grain size explains this scatter. Indeed, gravels are broadly distributed in size, and unevenly distributed over the river bed (Guerit et al., 2014). Since the rescaling for slope involves the grain size d_s to the power of 5/4, whereas this exponent is only 1/4 for width and depth (Eqs. 6 to 8), we believe the grain-size dispersion impacts more strongly the rescaled slope than the rescaled width and depth.

The means for braided threads and meandering threads differ by less than a factor of two, much smaller than the standard deviation. Fitting lognormal distributions to our data, we find that the meandering and braided channels from Bayanbulak cannot be distinguished from each other, at the 95 % level of confidence. The depth and slope of the Balyanbulak streams are also not significantly different from the GBR ones. Only the width of the Bayanbulak streams is significantly larger than that of the GBR streams. We therefore conclude that, within the natural variability of our observation, meandering and braided streams are morphologically similar. Again, the use of d_{90} instead of d_{50} as a characteristic grain size does not alter this conclusion.

According to the rescaling Eqs. (6)–(8) the aspect ratio of a stream W/H should be naturally detrended (Fig. 8). Indeed, the correlation coefficient of aspect ratio and discharge is less than 0.1 for all datasets (Table 2). As expected, the aspect ratio of braided and meandering threads cannot be distinguished at the 95 % level of confidence. Finally, the difference between the width of the Bayanbulak streams and that of the GBR streams also appears in the distribution of aspect ratio: the Bayanbulak streams are significantly wider than the GBR ones.

7 Conclusion

Our measurements on gravel-bed streams in the Bayanbulak grassland reveal that braided threads are morphologically similar to meandering ones. Their size can be virtually detrended with respect to water discharge using the threshold theory. As a result, their aspect ratio is naturally detrended. These findings accord with recent observations in sand-bed streams (Gaurav et al., 2015).

The striking similarity between braided and meandering threads in gravel-bed and sand-bed rivers supports the view that fully-developed braided rivers are essentially a collection of threads interacting with each other, rather than a single wide channel rumpled by sediment bars. If confirmed, this would suggest that a braid results from the collective behavior of individual threads, the property and dynamics of which would be close to that of isolated channels.

Our observations, like those of Gaurav et al. (2015) and the GBR dataset, are much dispersed around their average value, which points at the influence of hidden parameters on their morphology. Among those, the intensity of sediment transport is likely to play a prominent role. More specifically, field observations suggest that a heavier sediment load tends to increase the aspect ratio of a stream, other things being equal (Smith and Smith, 1984; Tal and Paola, 2010; Metivier and Barrier, 2012). This proposition needs to be thoroughly tested against dedicated field measurements, which we believe should include both braided and meandering threads. Finally, if the sediment discharge is indeed the most prominent parameter after water discharge, its influence on the morphology of a channel should also manifest itself in laboratory experiments.

Acknowledgements. This paper is dedicated to the dear memory of Baisheng Ye. The Bayanbulak field campaign was the last we carried out together, before he accidentally died on assignment in Tibet. This work is under the aegis of the SALADYN international associated laboratory. It is IPGP contribution 3685.

References

Bertoldi, W. and Tubino, M.: River bifurcations: experimental observations on equilibrium configurations, Water Resour. Res., 43, W10437, doi:10.1029/2007WR005907, 2007.

Bolla Pittaluga, M., Repetto, R., and Tubino, M.: Channel bifurcation in braided rivers: equilibrium configurations and stability, Water Resour. Res., 39, 1046, doi:10.1029/2001WR001112, 2003.

Bunte, K. and Abt, S.: Sampling surface and subsurface particle-size distributions in wadable gravel- and cobble-bed streams for analyses in sediment transport, hydraulics, and streambed monitoring, Technical report, Gen. Tech. Rep. RMRS-GTR-74, Fort Collins,CO, US Department of Agriculture, Forest Service, Rocky Mountain Research Station, 428 pp., 2001. 1294

Church, M. and Gilbert, R.: Proglacial fluvial and lacustrine environments, in: Glaciofluvial and Glaciolacustrine Sedimentation, vol. 23 of Special Publication, SEPM, Tulsa, 22–100, 1975. 1292

Church, M. and Rood, K.: Catalogue of Alluvial River Channel Regime Data, Univ. British Columbia, Department of Geography, Vancouver, 1983. 1294, 1312

Devauchelle, O., Petroff, A., Lobkovsky, A., and Rothman, D. H.: Longitudinal profile of channels cut by springs, J. Fluid Mech., 667, 38–47, 2011.

Fredsøe, J.: Meandering and braiding of rivers, J. Fluid Mech., 84, 609–624, 1978. 1291, 1292

Gaurav, K., Métivier, F., Devauchelle, O., Sinha, R., Chauvet, H., Houssais, M., and Bouquerel, H.: Morphology of the Kosi megafan channels, Earth Surf. Dynam., 3, 321–331, doi:10.5194/esurf-3-321-2015, 2015. 1292, 1294, 1296, 1299, 1300

Glover, R. E. and Florey, Q.: Stable Channel Profiles, US Department of the Interior, Bureau of Reclamation, Design and Construction Division, Denver Colorado, 1951. 1292, 1296, 1297

Gran, K. and Paola, C.: Riparian vegetation controls on braided stream dynamics, Water Resour. Res., 37, 3275–3283, 2001. 1292

Guerit, L., Barrier, L., Narteau, C., Métivier, F., Liu, Y., Lajeunesse, E., Gayer, E., Meunier, P., Malverti, L., and Ye, B.: The Grain-size Patchiness of Braided Gravel-Bed Streams – example of the Urumqi River (northeast Tian Shan, China), Adv. Geosci., 37, 27–39, doi:10.5194/adgeo-37-27-2014, 2014. 1298

Henderson, F. M.: Stability of alluvial channels, T. Am. Soc. Civ. Eng., 128, 657–686, 1963. 1292, 1296, 1297

Hey, R. D. and Thorne, C. R.: Stable channels with mobile gravel beds, J. Hydraul. Eng.-ASCE, 112, 671–689, 1986. 1293

King, J. G., Emmett, W. W., Whiting, P. J., Kenworthy, R. P., and Barry, J. J.: Sediment transport data and related information for selected coarse-bed streams and rivers in Idaho, Gen. Tech. Rep. RMRS-GTR-131, Fort Collins, CO, RMRS-GTR-131, U.S. Department of Agriculture, Forest Service, Rocky Mountain Research Station, Fort Collins, CO, 2004. 1294, 1312

Mackin, H.: Concept of the graded river, Bull. Geol. Soc. Am., 59, 463–512, 1948.

Metivier, F. and Barrier, L.: Alluvial landscape evolution: what do we know about metamorphosis of gravel bed meandering and braided streams, in: Gravel-Bed Rivers: Processes, Tools, Environments, edited by: Church, M., Biron, P., and Roy, A., chapter 34, 474–501, Wiley & Sons, Chichester, 2012. 1292, 1297, 1300

Mosley, M.: Response of braided rivers to changing discharge, Journal of Hydrology New Zealand, 22, 18–67, 1983. 1292

Paola, C.: Modelling stream braiding over a range of scales, in: Gravel Bed Rivers V, 11–46, New Zealand hydrologic society, Wellington, 2001.

Parker, G.: On the cause and characteristic scales of meandering and braiding in rivers, J. Fluid Mech., 76, 457–480, 1976. 1291, 1292

Parker, G.: Transport of gravel and sand mixtures, in: Sedimentation Engineering: Processes, Management, Modeling, and Practice, edited by: Garcia, M. H., Vol. 110, chapter 3, 165–251, ASCE, Reston, 2008. 1295

Parker, G., Wilcock, P., Paola, C., Dietrich, W. E., and Pitlick, J.: Quasi-universal relations for bankfull hydraulic geometry of single-thread gravel-bed rivers, J. Geophys. Res.-Earth, 112, 1–21, 2007. 1294, 1295, 1297, 1312

Reitz, M. D., Jerolmack, D. J., Lajeunesse, E., Limare, A., Devauchelle, O., and Métivier, F.: Diffusive evolution of experimental braided rivers, Phys. Rev. E, 89, 052809, doi:10.1103/PhysRevE.89.052809, 2014. 1292

Sanders, L.: A Manual of Field Hydrogeology, Prentice-Hall, Inc., Englewood Cliffs, NJ, USA, 1998. 1294

Scherrer, B.: Biostatistique, G. Morin, Chicoutimi, Québec, 1984. 1295

Schumm, S. A.: River Variability and Complexity, Cambridge Univ. Pr., Cambridge, UK, 2005. 1291

Seizilles, G.: Forme d’équilibre d’une rivière, PhD thesis, Université Paris Diderot, Paris, France, 2013. 1296

Seizilles, G., Devauchelle, O., Lajeunesse, E., and Métivier, F.: Width of laminar laboratory rivers, Phys. Rev. E, 87, 052204, doi:10.1103/PhysRevE.87.052204, 2013. 1292, 1297

Smith, N. D. and Smith, D. G.: William River: an outstanding example of channel widening and braiding caused by bed-load addition, Geology, 12, 78–82, 1984. 1292, 1300

Sokal, R. and Rohlf, F.: Biometry, W. H. Freeman, New York, 1995. 1295

Tal, M. and Paola, C.: Dynamic single-thread channels maintained by the interaction of flow and vegetation, Geology, 35, 347–350, doi:10.1130/G23260A.1, 2007. 1292

Tal, M. and Paola, C.: Effects of vegetation on channel morphodynamics: results and insights from laboratory experiments, Earth Surf. Proc. Land., 35, 1014–1028, 2010. 1292, 1300

Yalin, M. S. and Ferreira da Silva, A. M.: Fluvial Processes, International Association of Hydraulic Engineering and Research Monograph, Delft, 2001. 1296

Yang, Q. and Cui, C.: Impact of climate change on the surface water of kaidu river basin, J. Geogr. Sci., 15, 20–28, 2005. 1293

Zhang, B., Yao, Y.-H., Cheng, W.-M., Zhou, C., Lu, Z., Chen, X., Alshir, K., ErDowlet, I., Zhang, L., and Shi, Q.: Human-induced changes to biodiversity and alpine pastureland in the bayanbulak region of the east tienshan mountains, Mt. Res. Dev., 22, 383–389, 2002. 1293

Zhang, Y., Li, B., Bao, A., Zhou, C., Chen, X., and Zhang, X.: Study on snowmelt runoff simulation in the kaidu river basin, Sci. China Ser. D, 50, 26–35, 2007. 1293

Zolezzi, G., Bertoldi, W., and Tubino, M.: Morphological analysis and prediction of river bifurcations, in: Braided Rivers: Process, Deposits, Ecology and Management, Special Publication 36 of the IAS, 36, 233–256, Blackwell Publishing Ltd, Oxford, UK, 2006.

Zolezzi, G., Bertoldi, W., and Tubino, M.: Morphodynamics of bars in gravel-bed rivers: bridging analytical models and field observations, in: Gravel-Bed Rivers: Processes, Tools, Environments, 69–89, Wiley-Blackwell, Chichester, UK, 2012. 1291, 1292

Table 1. Linear regressions on the $\log_{10}$ of width and depth as functions of discharge and for two characteristic grain sizes. Confidence level is 95 %. RMA: Reduced major axis regression σ_β stands for confidence interval on the slope of the regression β.

Width: $\log_{10}(W/d_s) = \beta_\mathrm{w}\log_{10}Q_* + \alpha_\mathrm{w}$

Thread	d_s	β_w	α_w	$\sigma_{\beta_\mathrm{w}}$	R^2
Total Pop.	d_{50}	0.33	1.47	0.03	0.83
	d_{90}	0.34	1.35	0.04	0.78
Meandering	d_{50}	0.35	1.38	0.04	0.91
	d_{90}	0.33	1.37	0.04	0.91
Braided	d_{50}	0.32	1.51	0.05	0.78
	d_{90}	0.35	1.34	0.07	0.66
GBR	d_{50}	0.43	0.89	0.02	0.79
	d_{90}	0.49	0.78	0.04	0.94

Depth: $\log_{10}(H/d_s) = \beta_\mathrm{h}\log_{10}Q_* + \alpha_\mathrm{h}$

Thread type	d_s	β_h	α_h	$\sigma_{\beta_\mathrm{h}}$	R^2
Total Pop.	d_{50}	0.44	−0.62	0.04	0.84
	d_{90}	0.4	−0.5	0.05	0.77
Meandering	d_{50}	0.44	−0.66	0.08	0.84
	d_{90}	0.39	−0.46	0.08	0.8
Braided	d_{50}	0.44	−0.61	0.05	0.83
	d_{90}	0.41	−0.51	0.07	0.7
GBR	d_{50}	0.41	−0.34	0.02	0.81
	d_{90}	0.34	−0.29	0.04	0.9

Table 2. Mean and standard deviations of the logarithms of detrended widths, depths and slopes. The aspect ratios is naturally detrended and does not depend on grain size. The difference for the GBR dataset comes from the size of the sample that is different for the two grain sizes.

Width $\log_{10}(W_*)$			
River type	Grain size	Mean	Standard deviation
Meandering	D_{50}	0.6	0.3
Meandering	D_{90}	0.8	0.2
Braided	D_{50}	0.7	0.3
Braided	D_{90}	0.8	0.2
GBR	D_{50}	0.2	0.2
GBR	D_{90}	0.5	0.1
Depth $\log_{10}(H_*)$			
River type	Grain size	Mean	Standard deviation
Meandering	D_{50}	−0.1	0.3
Meandering	D_{90}	−0.0	0.3
Braided	D_{50}	−0.2	0.2
Braided	D_{90}	−0.1	0.2
GBR	D_{50}	−0.2	0.1
GBR	D_{90}	−0.0	0.2
Slope $\log_{10}(S_*)$			
River type	Grain size	Mean	Standard deviation
Meandering	D_{50}	0.4	0.7
Meandering	D_{90}	−0.22	0.74
Braided	D_{50}	0.5	0.7
Braided	D_{90}	−0.11	0.46
GBR	D_{50}	0.7	0.4
GBR	D_{90}	−0.05	0.24
Aspect Ratio $\log_{10}(W/H)$			
River type	Grain size	Mean	Standard deviation
Meandering	–	1.6	0.3
Braided	–	1.7	0.4
GBD	D_{50}	1.3	0.2
GBD	D_{90}	1.4	0.3

Table 3. Data gathered for braided threads. Latitude (lat) and longitude (lon) are in degrees centesimal; Measurement stands for measurement type (Fl: float, ADCP: Acoustic doppler curent profiler); Q: Discharge, Sec: wetted area, V: average velocity, W: width, H: Depth, D_{50}: median grain size, D_{90}: size of the 90th percentile, S: slope. All physical quantities are given in SI units.

Code	Lat	Lon	Channel	Measurement	Q	Sec	V	W	H	D_{50}	D_{90}	S
174	42.7611	83.841	B	Fl	2.9	2.6	1.1	18.0	0.14	0.028	0.064	0.0044
180	42.7617	83.8428	B	Fl	4.2	2.3	1.8	17.0	0.14	0.028	0.064	0.012
181	42.7602	83.8454	B	Fl	1.1	1.8	0.62	14.0	0.13	0.028	0.064	0.0064
182	42.7604	83.8448	B	Fl	0.36	0.52	0.69	7.0	0.073	0.028	0.064	0.01
183	42.7617	83.8439	B	Fl	0.73	1.4	0.52	10.0	0.14	0.028	0.064	0.0079
184	42.7609	83.8417	B	Fl	0.62	0.74	0.84	18.0	0.041	0.028	0.064	0.0092
185	42.7608	83.8415	B	Fl	2.4	1.9	1.2	11.0	0.19	0.028	0.064	0.013
168	42.7307	84.5878	B	Fl	0.0034	0.011	0.32	1.7	0.0062	0.027	0.064	0.043
142	42.9985	83.943	B	Fl	0.025	0.11	0.23	1.5	0.074	0.013	0.064	0.012
141	43.0004	83.9435	B	Fl	0.38	1.0	0.38	4.9	0.2	0.013	0.064	0.012
139	42.9985	83.943	B	Fl	0.41	0.9	0.46	4.0	0.23	0.013	0.064	0.012
137	43.0004	83.9435	B	Fl	0.099	0.24	0.41	1.9	0.13	0.013	0.064	0.012
179	42.7618	83.8416	B	Fl	0.84	0.96	0.87	11.0	0.089	0.028	0.064	0.008
178	42.7609	83.8413	B	Fl	0.097	0.25	0.39	16.0	0.015	0.028	0.064	0.0092
173	42.7622	83.8404	B	Fl	0.56	1.9	0.3	18.0	0.1	0.028	0.064	0.0027
172	42.7605	83.8447	B	Fl	0.21	0.28	0.72	5.3	0.054	0.028	0.064	0.0073
171	42.7608	83.8446	B	Fl	0.26	0.5	0.52	7.5	0.066	0.028	0.064	0.0077
170	42.7619	83.8416	B	Fl	1.9	3.1	0.62	17.0	0.18	0.028	0.064	0.0098
169	42.7316	84.5874	B	Fl	0.23	0.9	0.26	8.8	0.1	0.027	0.064	0.0014
175	42.7604	83.8452	B	Fl	0.084	0.21	0.41	6.9	0.03	0.028	0.064	0.0097
167	42.7314	84.5877	B	Fl	0.0025	0.017	0.15	1.2	0.014	0.027	0.064	0.02
166	42.731	84.5877	B	Fl	0.015	0.076	0.2	2.8	0.027	0.027	0.064	0.015
165	42.7305	84.5887	B	Fl	0.04	0.18	0.22	3.6	0.05	0.027	0.064	0.0034
176	42.7609	83.8419	B	Fl	3.5	2.9	1.2	13.0	0.23	0.028	0.064	0.0062
177	42.7623	83.8404	B	Fl	0.053	0.13	0.4	2.2	0.06	0.028	0.064	0.016
135	43.0004	83.9435	B	Fl	0.018	0.11	0.17	2.1	0.05	0.013	0.064	0.012

Table 3. Continued.

Code	Lat	Lon	Channel	Measurement	Q	Sec	V	W	H	D_{50}	D_{90}	S
134	42.9985	83.943	B	Fl	0.044	0.13	0.33	1.5	0.09	0.013	0.064	0.012
125	42.7995	83.8983	B	Fl	0.19	0.44	0.43	4.9	0.09	0.013	0.053	0.008
111	42.7898	83.9064	B	Fl	0.03	0.071	0.43	2.0	0.036	0.013	0.053	0.008
112	42.7944	83.9025	B	Fl	1.9	2.6	0.71	4.9	0.54	0.013	0.053	0.008
113	42.7946	83.9025	B	Fl	0.14	0.29	0.47	2.8	0.1	0.013	0.053	0.008
114	42.7985	83.8993	B	Fl	1.0	1.7	0.61	6.2	0.27	0.013	0.053	0.008
115	42.799	83.8992	B	Fl	0.15	0.29	0.53	2.0	0.14	0.013	0.053	0.008
116	42.7924	83.904	B	Fl	0.0056	0.018	0.3	0.6	0.031	0.013	0.053	0.008
117	42.7911	83.9053	B	Fl	0.02	0.083	0.24	2.1	0.04	0.013	0.053	0.008
118	42.7991	83.8989	B	Fl	0.39	0.81	0.48	4.8	0.17	0.013	0.053	0.008
110	42.7983	83.8995	B	Fl	0.68	0.91	0.74	4.9	0.19	0.013	0.053	0.008
109	42.7914	83.905	B	Fl	0.14	0.35	0.39	4.4	0.08	0.013	0.053	0.008
101	42.7915	83.905	B	Fl	0.71	1.1	0.66	9.3	0.12	0.013	0.053	0.008
102	42.7921	83.9042	B	Fl	0.91	1.9	0.47	9.4	0.2	0.013	0.053	0.008
103	42.7944	83.9025	B	Fl	0.04	0.1	0.39	3.0	0.034	0.013	0.053	0.008
104	42.7946	83.9025	B	Fl	0.093	0.16	0.59	3.0	0.053	0.013	0.053	0.008
105	42.7916	83.9047	B	Fl	0.014	0.066	0.21	3.6	0.018	0.013	0.053	0.008
106	42.7985	83.8994	B	Fl	0.08	0.38	0.21	8.3	0.045	0.013	0.053	0.008
107	42.7983	83.8994	B	Fl	0.76	1.1	0.7	5.8	0.19	0.013	0.053	0.008
108	42.7898	83.9063	B	Fl	1.1	1.4	0.74	8.0	0.18	0.013	0.053	0.008
119	42.7925	83.9037	B	Fl	0.017	0.06	0.29	1.2	0.05	0.013	0.053	0.008
100	42.7925	83.9037	B	Fl	0.085	0.23	0.38	2.2	0.1	0.013	0.053	0.008
124	42.7934	83.903	B	Fl	0.5	1.2	0.4	6.5	0.19	0.013	0.053	0.008
123	42.7884	83.907	B	Fl	0.072	0.33	0.22	3.9	0.083	0.013	0.053	0.008
122	42.7926	83.9037	B	Fl	0.68	1.1	0.64	4.3	0.25	0.013	0.053	0.008
121	42.7937	83.9028	B	Fl	1.5	2.2	0.66	9.3	0.24	0.013	0.053	0.008
120	42.7953	83.9025	B	Fl	0.33	1.1	0.29	5.2	0.22	0.013	0.053	0.008
646	42.6926	83.6944	B	ADCP	51.0	24.0	2.2	35.0	0.68	0.011	0.15	0.012
649	42.6926	83.6944	B	ADCP	33.0	17.0	2.0	27.0	0.62	0.011	0.15	0.012
652	42.6926	83.6944	B	ADCP	26.0	14.0	1.9	23.0	0.59	0.011	0.15	0.012
655	42.6926	83.6944	B	ADCP	38.0	19.0	2.0	31.0	0.62	0.011	0.15	0.012

Table 4. Data gathered for meandering and straight threads. Latitude (lat) and longitude (lon) are in degrees centesimal; Measurement stands for measurement type (Fl: float, ADCP: Acoustic doppler curent profiler); Q: Discharge, Sec: wetted area, V: average velocity, W: width, H: Depth, D_{50}: median grain size, D_{90}: size of the 90th percentile, S: slope. All physical quantities are given in SI units.

Code	Lat	Lon	Channel	Measurement	Q	Sec	V	W	H	D_{50}	D_{90}	S
614	42.8229	83.9253	M	ADCP	0.69	2.1	0.33	7.3	0.28	0.007	0.038	0.0021
626	42.8915	83.835	M	ADCP	8.2	6.5	1.3	23.0	0.28	0.013	0.03	0.0016
609	42.8227	83.9366	M	ADCP	1.1	1.9	0.56	9.5	0.2	0.007	0.038	0.0021
625	42.8915	83.835	M	ADCP	8.9	6.7	1.3	23.0	0.29	0.013	0.03	0.0016
610	42.8227	83.9366	M	ADCP	1.2	2.0	0.59	9.5	0.21	0.007	0.038	0.0021
624	42.8915	83.835	M	ADCP	7.9	6.2	1.3	20.0	0.31	0.013	0.03	0.0016
611	42.8227	83.9366	M	ADCP	1.1	2.4	0.46	8.1	0.3	0.007	0.038	0.0021
612	42.8227	83.9366	M	ADCP	1.2	2.5	0.46	8.0	0.32	0.007	0.038	0.0021
623	42.8915	83.835	M	ADCP	8.7	6.8	1.3	21.0	0.33	0.013	0.03	0.0016
613	42.8229	83.9253	M	ADCP	0.74	2.2	0.34	7.5	0.29	0.007	0.038	0.0021
617	42.8229	83.9253	M	ADCP	0.42	0.97	0.43	7.9	0.12	0.007	0.038	0.0021
616	42.8229	83.9253	M	ADCP	0.4	0.96	0.42	7.8	0.12	0.007	0.038	0.0021
615	42.8229	83.9253	M	ADCP	0.73	2.2	0.33	7.6	0.29	0.007	0.038	0.0021
608	42.8227	83.9366	M	ADCP	0.63	1.2	0.51	8.2	0.15	0.007	0.038	0.0021
144	43.0224	83.9376	M	Fl	0.53	1.3	0.4	6.6	0.2	0.013	0.064	0.012
151	42.9721	84.0495	M	Fl	0.0076	0.046	0.16	1.9	0.024	0.009	0.034	0.01
150	42.9901	84.0785	M	Fl	0.3	0.32	0.94	3.6	0.088	0.02	0.014	0.026
149	42.9902	84.0764	M	Fl	0.3	0.34	0.88	3.9	0.088	0.02	0.014	0.026
148	42.9925	84.0758	M	Fl	0.37	0.42	0.87	4.4	0.096	0.02	0.014	0.026
147	42.9909	84.0781	M	Fl	0.29	0.35	0.82	4.7	0.074	0.02	0.014	0.026
146	42.9679	84.0473	M	Fl	0.18	0.16	1.1	2.6	0.061	0.016	0.04	0.012
145	42.9682	84.0468	M	Fl	0.2	0.23	0.87	3.1	0.075	0.016	0.04	0.012
143	43.0206	83.9402	M	Fl	0.5	1.1	0.45	4.9	0.23	0.013	0.064	0.012
140	43.0167	83.9418	M	Fl	0.5	1.4	0.37	4.4	0.31	0.013	0.064	0.012
138	43.0059	83.945	M	Fl	0.47	1.6	0.29	8.0	0.21	0.013	0.064	0.012
136	43.011	83.9416	M	Fl	0.52	1.4	0.39	5.7	0.24	0.013	0.064	0.012
152	42.9713	84.049	M	Fl	0.0088	0.053	0.17	2.3	0.023	0.009	0.034	0.01
153	42.9751	84.0496	M	Fl	0.0088	0.052	0.17	1.4	0.037	0.009	0.034	0.01
164	42.8769	84.0626	M	Fl	0.52	7.4	0.07	9.3	0.8	0.015	0.034	0.00015
163	42.8895	84.0873	M	Fl	0.012	0.1	0.11	4.2	0.025	0.015	0.034	0.002
162	42.8881	84.0782	M	Fl	0.14	1.3	0.11	6.7	0.19	0.015	0.034	0.0012
161	42.8812	84.0603	M	Fl	1.0	6.7	0.15	9.3	0.72	0.015	0.034	0.00015
160	42.8887	84.0836	M	Fl	0.071	0.74	0.095	4.7	0.16	0.015	0.034	0.0017
159	42.889	84.0881	M	Fl	0.0029	0.083	0.035	1.4	0.059	0.015	0.034	0.002
158	42.8852	84.0688	M	Fl	0.31	2.8	0.11	9.5	0.29	0.015	0.034	0.0005
157	42.889	84.0861	M	Fl	0.035	0.52	0.068	3.6	0.14	0.015	0.034	0.002
156	42.8891	84.088	M	Fl	0.0048	0.29	0.017	2.1	0.14	0.015	0.034	0.002
155	42.9733	84.0494	M	Fl	0.0084	0.017	0.49	1.8	0.0099	0.009	0.034	0.01
154	42.9686	84.0489	M	Fl	0.0097	0.027	0.36	2.9	0.0093	0.009	0.034	0.01

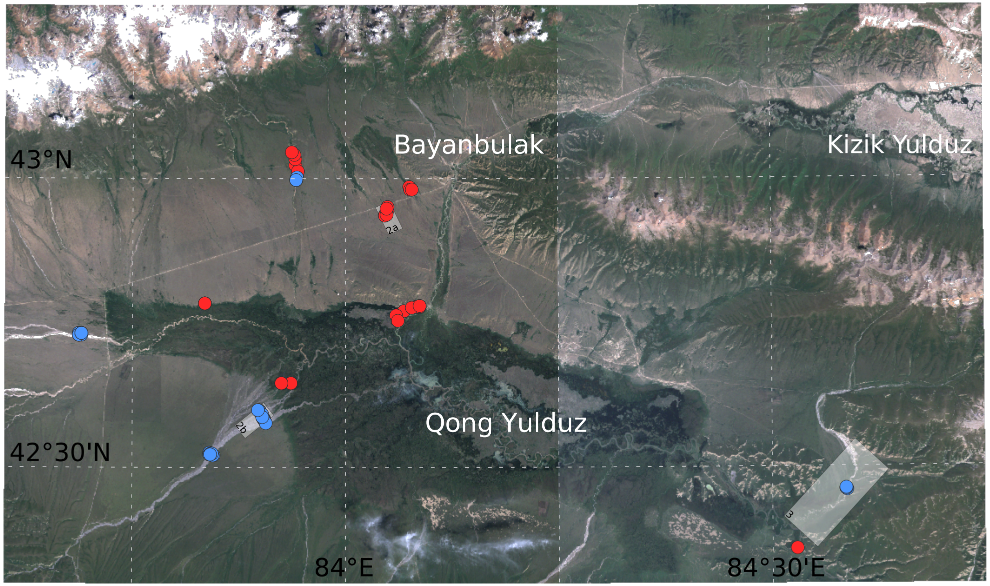

Figure 1. Satellite image of the Bayanbulak Grassland (Landsat 5 mosaic). Red (meandering) and blue (braided) dots indicate measurement sites. White rectangles correspond to Figs. 2 and 3.

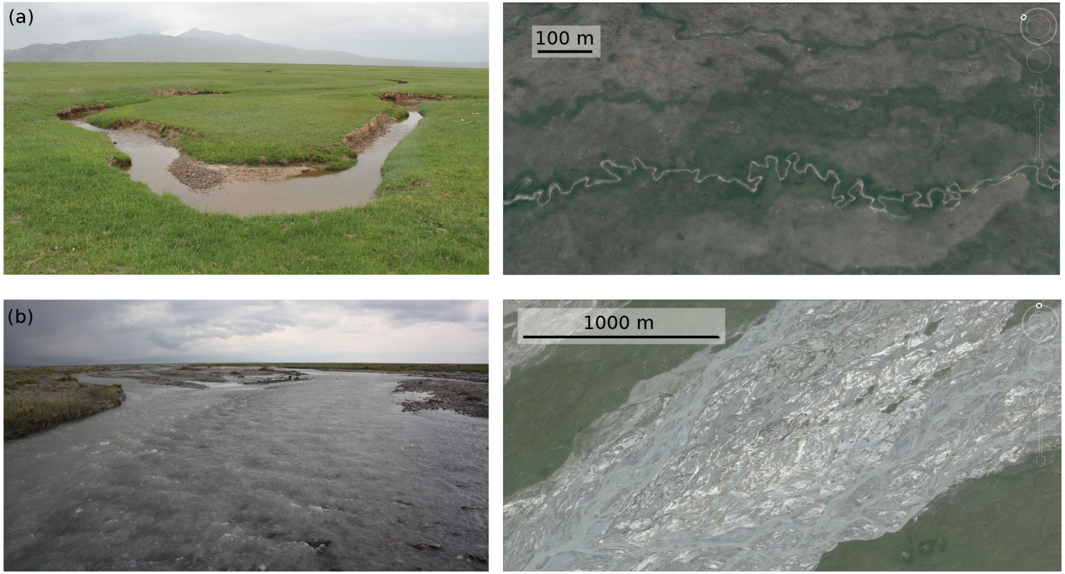

Figure 2. (a) Meandering and **(b)** braided streams in the Bayanbulak Grassland. Left: field picture; right: satellite image (Google Earth). The corresponding locations also appear in Fig. 1.

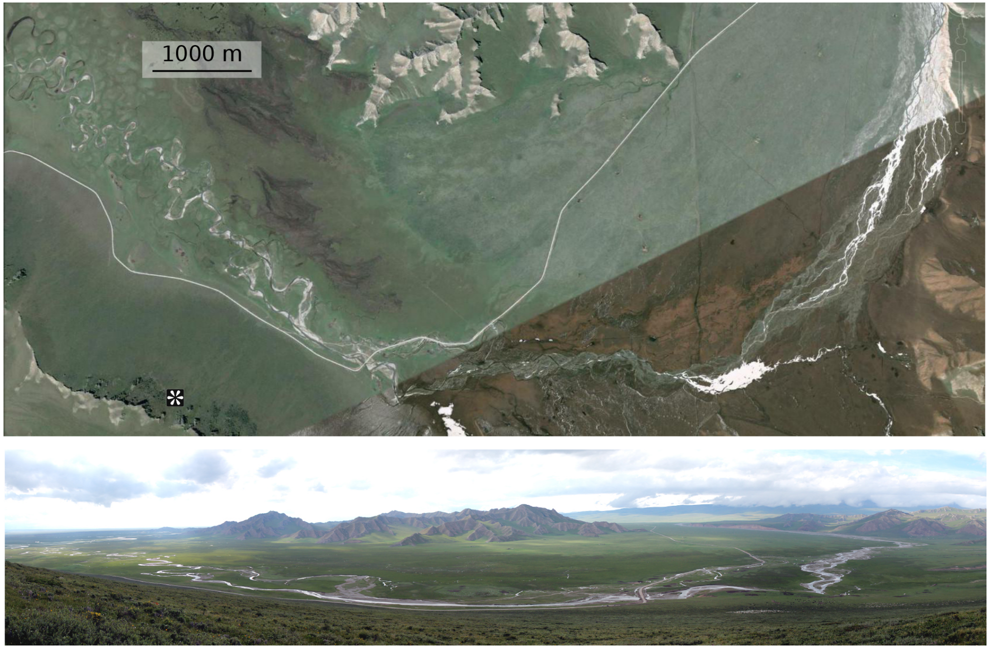

Figure 3. Satellite and panoramic view of a metamorphosis from braided to meandering (Bayanbulak Grassland, 84.578° E, 42.721° N, Google Earth). Marker on the satellite image indicates the viewpoint of the panoramic image. Its location also appears in Fig. 1.

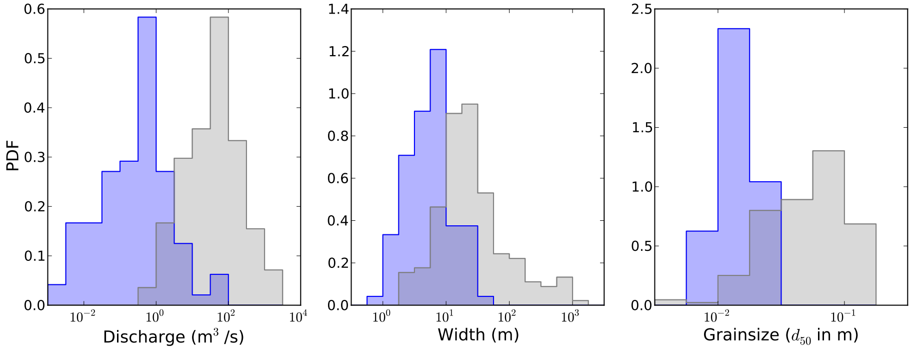

Figure 4. Normed histograms (probability density function) of water discharge, width and grain size. Blue: this study; gray: GBR dataset (Church and Rood, 1983; Parker et al., 2007; King et al., 2004).

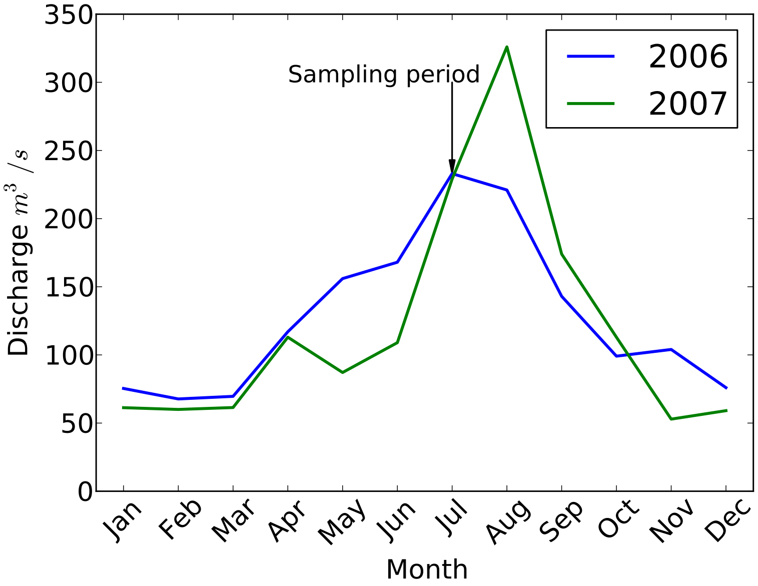

Figure 5. Water discharge of the Kaidu River at the Dashankou station, downstream of the grassland (monthly average). Source: Xinjiang Insitute for Ecology and Geography.

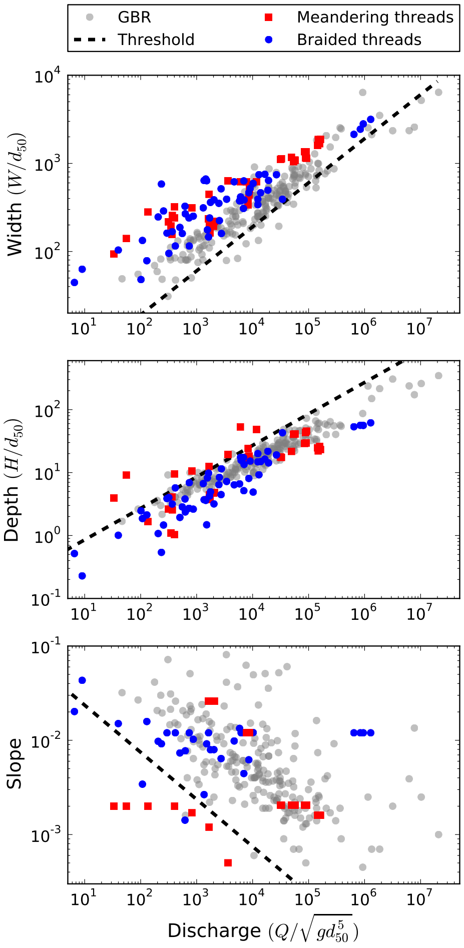

Figure 6. Dimensionless width, depth and slope of individual gravel-bed threads as a function of dimensionless water discharge. Dashed lines represent the threshold theory.

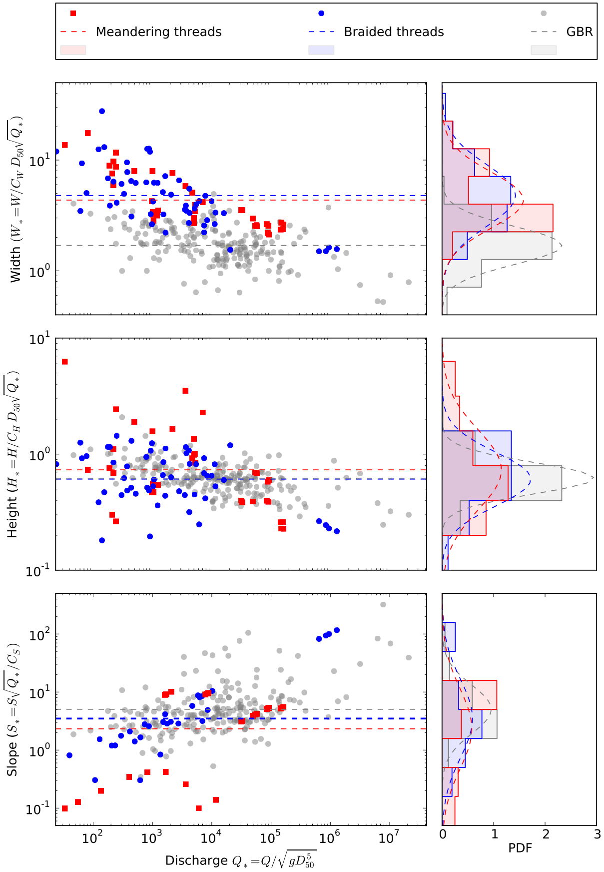

Figure 7. Left: rescaled width (W_*), depth (H_*) and slope (S_*) as a function of rescaled water discharge (Q_*). Rescaled quantities are from Eqs. (6)–(8). Threshold streams correspond to rescaled width, depth and slope equal to 1. Right: probability density function of rescaled quantities, with fitted lognormal distributions.

ESURFD

3, 1289–1316, 2015

Braided and meandering threads

F. Métivier et al.

Title Page
Abstract
Introduction
Conclusions
References
Tables
Figures
◀▎
▶▎
◀
▶
Back
Close
Full Screen / Esc
Printer-friendly Version
Interactive Discussion

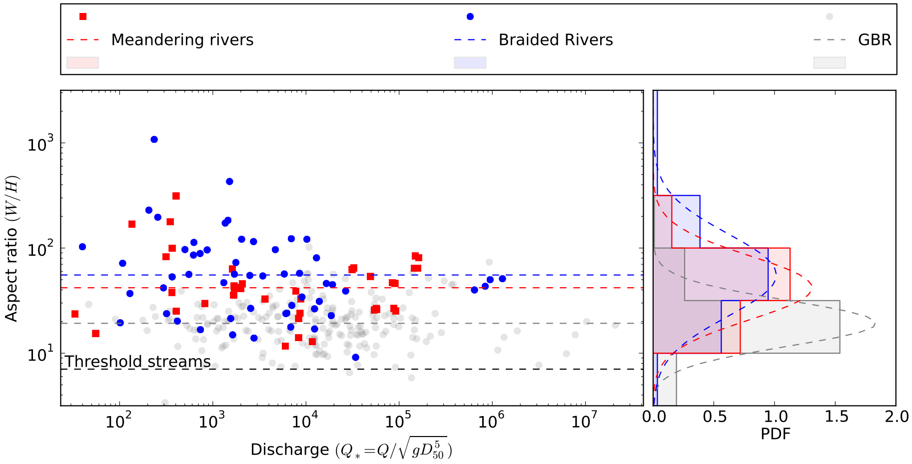

Figure 8. Aspect ratio of braided and meandering threads from Bayanbulak and isolated streams from the GBR datasets, as a function of rescaled water discharge (Q_*).

Title Page
Abstract | Introduction
Conclusions | References
Tables | Figures
◀▮ | ▶▮
◀ | ▶
Back | Close
Full Screen / Esc
Printer-friendly Version
Interactive Discussion